OFDM-Based Generalized Spatial Modulation for Optical Wireless Communication

Xin Zhong[1], Chen Chen[1,*], Shu Fu[1], Xin Jian[1], Min Liu[1], and Xiong Deng[2]
[1]School of Microelectronics and Communication Engineering
Chongqing University, Chongqing 400044, China
[2]Department of Electrical Engineering
Eindhoven University of Technology (TU/e), 5600MB Eindhoven, Netherlands
[*]c.chen@cqu.edu.cn

2021 IEEE 16th Conference on Industrial Electronics and Applications (ICIEA) | 978-1-6654-2248-2/21/$31.00 ©2021 IEEE | DOI: 10.1109/ICIEA51954.2021.9516223

***Abstract*—In this paper, we propose two orthogonal frequency division multiplexing (OFDM)-based generalized spatial modulation (GSM) techniques, i.e., frequency domain GSM (FD-GSM) and time domain GSM (TD-GSM), for indoor multiple-input multiple-output optical wireless communication (MIMO-OWC) systems. Specifically, FD-GSM selects a subset of parallel OFDM modulators to transmit the same quadrature amplitude modulation (QAM) constellation symbol in the subcarrier level, while TD-GSM selects a subset of light-emitting diode (LED) transmitters to transmit the same time domain sample after OFDM modulation. Compared with the existing OFDM-based spatial modulation (SM) scheme, OFDM-based GSM can provide additional transmit diversity. For both FD-GSM and TD-GSM, maximum-likelihood (ML) detectors are employed to recover the spatial and constellation symbols. Moreover, TD-GSM usually requires a secondary direct current (DC) bias to work properly. The simulation results show that in a typical indoor 4×4 MIMO-OWC system, OFDM-based TD-GSM outperforms OFDM-based FD-GSM by adding a proper secondary DC bias.**

***Index Terms*—Optical wireless communication (OWC), multiple-input multiple-output (MIMO), generalized spatial modulation (GSM).**

I. Introduction

RCENTLY, the involvement of new technologies such as virtual/augmented reality (VR/AR), Internet of things (IoT) and artificial intelligence (AI) results in higher demand for data rates. Due to the exhaustion of radio frequency (RF) spectrum resources, the utilization of high frequency resources becomes a development trend. In the fifth generation (5G) wireless systems, the wireless communication industry has responded to this challenge by considering millimeter-wave, sub-6 GHz and the optical spectrum [1]. Among them, optical wireless communication (OWC) using infrared, visible light or ultra-violet light-emitting diodes (LEDs) has been considered as a promising candidate to satisfy the ever-increasing data demand in indoor environments. OWC systems have many attractive advantages such as license-free spectrum, high data rate, inherent physical-layer security and no electromagnetic interference [2]. Since the light emitted by LEDs is generally not coherent, typical OWC systems adopt intensity modulation with direct detection (IM/DD). Nevertheless, LEDs usually have a small electrical bandwidth, which greatly limit the achievable capacity of OWC systems.

This work was supported by the National Natural Science Foundation of China under Grant 61901065.

To improve the capacity of bandlimited OWC systems, many capacity-enhancing techniques have been proposed in the literature. Among them, multiple-input multiple-output (MIMO) transmission is one of the most popular techniques, which can provide substantial diversity or multiplexing gain for OWC systems [3]–[5]. There are mainly three types of MIMO schemes that have been applied in OWC systems for achieving diversity or multiplexing gains, including repetition coding (RC), spatial modulation (SM) and spatial multiplexing (SMP) [4], [6]. Although RC can provide substantial diversity gain, its spectral efficiency is low. In contrast, SMP can achieve high spectral efficiency, but suffers from severe inter-channel interference. SM has been shown to be a promising MIMO scheme, which can be seen as the combination of MIMO and digital modulation [7]. Nevertheless, it is challenging for SM to achieve high spectral efficiency [8]. In order to enhance the spectral efficiency of conventional SM, generalized SM (GSM) has been further proposed in [9], which can transmit the same symbol from more than one transmit antenna. Moreover, as a multi-carrier modulation technology, orthogonal frequency division multiplexing (OFDM) can make full use of limited bandwidth, and hence OFDM can be combined with SM to enhance the capacity of SM-based OWC systems. Generally, OFDM-based SM for OWC systems can be divided into two categories: one is OFDM-based frequency domain SM (FD-SM) and the other is OFDM-based time domain SM (TD-SM) [10], [11]. To the best of our knowledge, the combination of OFDM with GSM has not yet been considered for of OWC systems.

In this paper, we propose two OFDM-based GSM techniques for indoor MIMO-OWC systems, including FD-GSM and TD-GSM. The superiority of OFDM-based GSM over OFDM-based SM in typical indoor MIMO-OWC systems has been verified by simulation results. The rest of this paper is organized as follows. In Section II, we describe the channel model of a typical MIMO-OWC system. The principle of OFDM-based GSM techniques is described in Section III. The simulation results are presented in Section IV. Finally, Section V concludes the paper.

978-1-6654-2248-2/21/$31.00 ©2021 IEEE

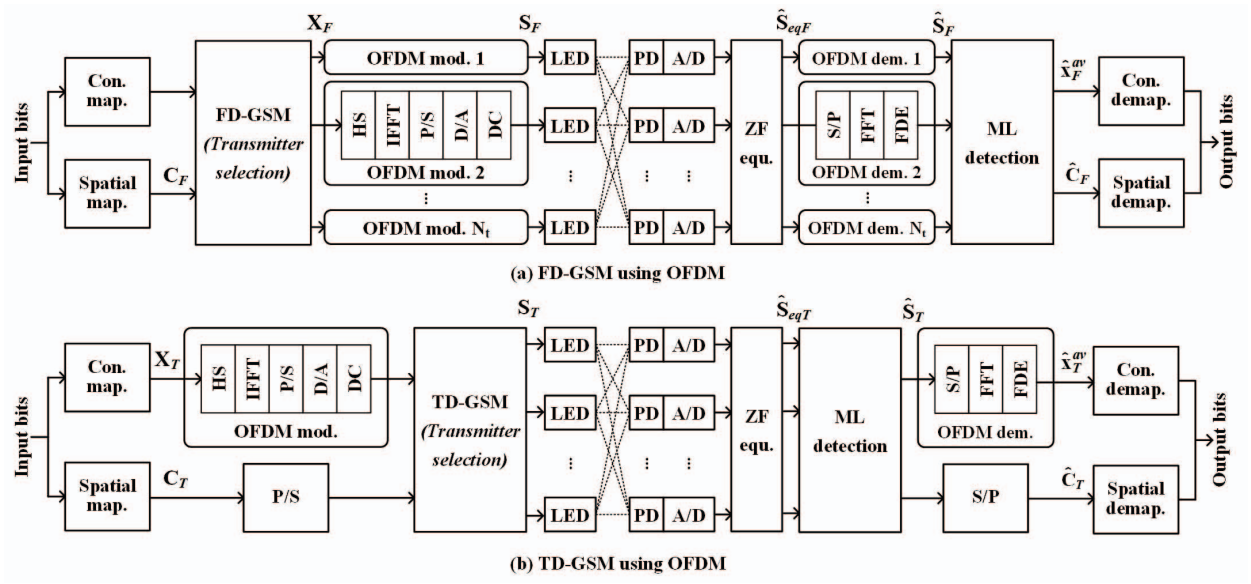

Fig. 1. Schematic diagrams of (a) OFDM-based FD-GSM and (b) OFDM-based TD-GSM.

II. MIMO Channel Model

In the following, we consider a typical MIMO-OWC system which consists of N_t LED transmitters and N_r photo-diodes (PDs). The received signal vector $\mathbf{y} = [y_1, y_2, \cdots, y_{N_r}]^T$ can be expressed by:

$$\mathbf{y} = \mathbf{H}\mathbf{s} + \mathbf{n}, \tag{1}$$

where $\mathbf{s} = [s_1, s_2, \cdots, s_{N_t}]^T$ is the transmitted signal vector and $\mathbf{n} = [n_1, n_2, \cdots, n_{N_r}]^T$ denotes noise vector, which can be assumed as a real-valued additive white Gaussian noise (AWGN) with zero mean and a variance σ^2. The noise power is $P_n = N_0 B_m$, where N_0 is the power spectral density (PSD) and B_m is the modulation bandwidth [4]. $\mathbf{H}$ represents the $N_r \times N_t$ MIMO channel matrix, where its element h_{rt} $(r = 1, \cdots, N_r; t = 1, \cdots, N_t)$ denotes the direct current channel gain between the r-th PD and the t-th LED. Assuming the LEDs follow the Lambertian radiation pattern and only considering the line-of-sight (LOS) component, h_{rt} can be calculated by:

$$h_{rt} = \frac{(l+1)\rho A}{2\pi d_{rt}^2} \cos^m(\varphi_{rt}) T_s(\theta_{rt}) g(\theta_{rt}) \cos(\theta_{rt}), \tag{2}$$

where $l = -\ln 2 / \ln(\cos(\Psi))$ is the Lambertian emission order, ρ and A are the responsivity and the active area of the PD, respectively; Ψ denotes the semi-angle at half power of the LED; d_{rt} is the distance between the r-th PD and the t-th LED; φ_{rt} and θ_{rt} are the emission angle and the incident angle, respectively; $T_s(\theta_{rt})$ is the gain of optical filter; $g(\theta_{rt}) = \frac{n^2}{\sin^2 \Phi}$ is the gain of optical lens, where n and Φ are the refractive index and the half-angle field-of-view (FOV) of the optical lens, respectively. If the incident light is outside the FOV of the receiver, h_{rt} becomes zero. At receiver side, zero forcing (ZF) equalization can be applied to recover the transmitted signal vector $\mathbf{s}$:

$$\hat{\mathbf{s}} = \mathbf{H}^{\dagger}\mathbf{y} = \mathbf{s} + \mathbf{H}^{\dagger}\mathbf{n}, \tag{3}$$

where $\mathbf{H}^{\dagger}$ is the pseudo inverse of $\mathbf{H}$.

III. OFDM-Based GSM Techniques

In this section, we first review the principle of OFDM for IM/DD OWC systems, and then describe the principle of the proposed two OFDM-based GSM techniques.

A. OFDM for IM/DD OWC

Due to the non-coherence nature of LEDs, IM/DD is generally adopted in OWC systems, and hence only real-valued non-negative signals can be successfully transmitted [12]. To generate IM/DD-compatible real-valued OFDM signals, the Hermitian symmetry constraint is usually imposed at the input of the N-pint inverse fast Fourier transform (IFFT) and hence resultant the input vector can be expressed by

$$\mathbf{X} = \left[0, X_1, \cdots, X_{N/2-1}, 0, X_{N/2-1}^*, \cdots, X_1^*\right]^T, \tag{4}$$

where X_k^* denotes the Hermitian conjugate of X_k with $k = 1, \cdots, N/2-1$. As we can see, due to the imposing of the Hermitian symmetry constraint, only $N/2-1$ subcarriers can be used for valid data transmission. A real-valued bipolar time-domain signal can be generated at the output of IFFT:

$$x_m = \frac{1}{\sqrt{N}} \sum_{k=0}^{N-1} X_m \exp\left(\frac{j2\pi km}{N}\right), m = 0, 1, \cdots, N-1. \tag{5}$$

For a relatively large value of N, x_m can be assumed to follow a Gaussian distribution with zero mean and variance σ^2. To obtain a non-negative signal to modulate the LEDs, the bipolar

TABLE I
MAPPING TABLE OF SPATIAL BITS FOR FD-GSM

Spatial bits	00	01	11	10
Spatial index vector	[1, 2]	[1, 3]	[2, 4]	[3, 4]
OFDM mod. 1	QAM	QAM	0	0
OFDM mod. 2	QAM	0	QAM	0
OFDM mod. 3	0	QAM	0	QAM
OFDM mod. 4	0	0	QAM	QAM

time-domain signal needs to be combined with a proper direct-current (DC) bias. Considering that OFDM signals usually have relatively high peak-to-average power ratio (PAPRs), soft clipping can be executed before adding the DC bias. Hence, the obtained non-negative time-domain signal is given by

$$s_m = \begin{cases} 0, & x_m < -b \\ x_m + b, & x_m \geq -b \end{cases}, \tag{6}$$

where $b = \alpha\sigma$ represents the added DC bias and α denotes the proportionality constant. Hence, we can define the DC bias in decibels as $b_{dB} = 10\log_{10}\left(\alpha^2 + 1\right)$.

B. OFDM-Based FD-GSM

Fig. 1(a) shows the block diagram of the $N_r \times N_t$ OFDM-based FD-GSM system. It can be seen that the input bits are first separated and then mapped into both constellation and spatial symbols. In OFDM-based FD-GSM, GSM is performed in the frequency domain, i.e., LED transmitter selection is carried out in the subcarrier level. The principle of FD-GSM is to select a subset of LED transmitters to transmit the same quadrature amplitude modulation (QAM) constellation symbol and the transmitter selection is determined by the corresponding spatial symbol. After performing FD-GSM, the resultant OFDM block matrix $\mathbf{X}_F$ can be given by

$$\mathbf{X}_F = \begin{bmatrix} x_{11} & \cdots & x_{1N} \\ \vdots & \ddots & \vdots \\ x_{N_t 1} & \cdots & x_{N_t N} \end{bmatrix}, \tag{7}$$

where OFDM modulation is performed for each row of $\mathbf{X}_F$.

For each column of $\mathbf{X}_F$, only a subset of the elements carry the same QAM symbol. Assuming N_a out of N_t elements in each column are selected to transmit the same QAM symbol, the number of total selection is obtained by $C(N_t, N_a)$, where $C(\cdot,\cdot)$ denotes the binomial coefficient. Table I illustrates the mapping table of spatial bits for FD-GSM with $N_t = 4$ and $N_a = 2$. As we can see, the spatial bits are mapped into a spatial index vector $[c_1, c_2]$, where c_1 and c_2 denote the spatial indexes of the two selected elements in each column, respectively. Note that FD-GSM becomes conventional FD-SM when $N_a = 1$ and FD-GSM becomes RC when $N_a = 4$.

After that, the OFDM block matrix is input into N_t OFDM modulation modules and the detailed principle of OFDM modulation can be found in [13]. Then, the output bipolar real-valued signals are transmitted by LEDs. Due to the use of Hermitian symmetry, only $\frac{N}{2} - 1$ subcarriers can be used for valid data transmission. Hence, the spectral efficiency of OFDM-based FD-GSM with N_t LEDs, N_a selected OFDM modulators and M-ary QAM constellation is given by:

$$\begin{aligned} SE_{\mathrm{FD-GSM}} &= \frac{\frac{N}{2} - 1}{N}\left(\log_2(M) + \lfloor \log_2\left(C(N_t, N_a)\right)\rfloor\right) \\ &\approx \underbrace{\frac{1}{2}\log_2(M)}_{\text{constellation}} + \underbrace{\frac{1}{2}\lfloor \log_2\left(C(N_t, N_a)\right)\rfloor}_{\text{spatial}}, \end{aligned} \tag{8}$$

where $\lfloor\cdot\rfloor$ denotes the floor operation. Subsequently, the received signals are equalized and further fed into OFDM demodulators. The output signal matrix $\hat{\mathbf{S}}_F$ is subsequently detected by a maximum-likelihood (ML) detector. The detailed procedures of ML detection are described in Algorithm 1. The moduli of the elements in $\hat{\mathbf{s}}_m$ $(m = 1, \cdots, N/2 - 1)$ are first calculated and then sorted in the descending order. Hence, we can obtain the sorted index vector $\mathbf{i} = [i_1, i_2, \cdots, i_{N_t}]^T$. Then, the first N_a elements of $\mathbf{i}$ are abstracted and an index vector $\mathbf{i}' = [i_1, i_2, \cdots, i_{N_a}]^T$ is obtained. By further sorting $\mathbf{i}'$ in the ascending order, we can obtain the sorted index vector $\hat{\mathbf{c}}_m = [\hat{c}_1, \cdots, \hat{c}_{N_a}]^T$ and the constellation symbol $\hat{\mathbf{x}}_m = [\hat{x}_{\hat{c}_1}, \cdots, \hat{x}_{\hat{c}_{N_a}}]^T$. Finally, the averaged signal $\hat{x}_m^{av} = \frac{1}{N_a}\sum_{i=1}^{N_a}\hat{x}_{\hat{c}_i}$ can be obtained.

Algorithm 1 ML detection for FD-GSM

Input: $\hat{\mathbf{S}}_F = [\hat{\mathbf{s}}_1, \cdots, \hat{\mathbf{s}}_{\frac{N}{2}-1}]$
Output: $\hat{\mathbf{C}}_F = [\hat{\mathbf{c}}_1, \cdots, \hat{\mathbf{c}}_{\frac{N}{2}-1}]$, $\hat{\mathbf{x}}_F^{av} = [\hat{x}_1^{av}, \cdots, \hat{x}_{\frac{N}{2}-1}^{av}]$
for $m = 1$ to $N/2 - 1$ **do**
  Calculate the moduli of the elements in $\hat{\mathbf{s}}_m$ and sort them in the descending order
  Obtain the sorted index vector $\mathbf{i} = [i_1, i_2, \cdots, i_{N_t}]^T$
  Abstract $\mathbf{i}' = [i_1, i_2, \cdots, i_{N_a}]^T$
  Sort the elements of $\mathbf{i}'$ in the ascending order
  Obtain the sorted index vector $\hat{\mathbf{c}}_m = [\hat{c}_1, \cdots, \hat{c}_{N_a}]^T$
  Obtain the constellation symbol $\hat{\mathbf{x}}_m = [\hat{x}_{\hat{c}_1}, \cdots, \hat{x}_{\hat{c}_{N_a}}]^T$
  Obtain the averaged signal $\hat{x}_m^{av} = \frac{1}{N_a}\sum_{i=1}^{N_a}\hat{x}_{\hat{c}_i}$
end for

C. OFDM-Based TD-GSM

Fig. 1(b) shows the block diagram of the $N_r \times N_t$ OFDM-based TD-GSM system. Compared with OFDM-based FD-GSM, GSM is performed in the time domain in OFDM-based TD-GSM and LED is selected after OFDM modulation. Hence, only N_a out of totally N_t LEDs are activated for valid data transmission and the others are just driven by DC biases for the purpose of illumination. The mapping table of spatial bits for OFDM-based TD-GSM is similar to that of OFDM-based FD-GSM, as shown in Table I, which is omitted here for brevity. Since GSM is performed in the time domain,the spatial symbol c_T is not constrained by the Hermitian symmetry and

TABLE II
SIMULATION PARAMETERS

Parameter	Value
Number of LEDs	4
Number of PDs	4
Room dimension	5 m × 5 m × 3 m
Height of ceiling	3 m
LED spacing	2.5m
Height of receiving plane	0.85 m
PD spacing	10 cm
Position of PDs	(2m, 2m, 0.85m)
Semi-angle at half power of LED	60°
Responsivity of the PD	1 A/W
Active area of PD	1 cm^2
Refractive index	1.5
Half-angle FOV of optical lens	72°
Noise PSD	10^{-22} A^2/Hz
Signal bandwidth	20 MHz
Gain of the optical filter	0.9
Number of activated LEDs	1,2,3,4

hence the spectral efficiency of OFDM-based TD-GSM can be obtained by

$$SE_{\text{TD-GSM}} = \frac{\frac{N}{2}-1}{N}\log_2(M) + \lfloor \log_2(N_t, N_a) \rfloor \approx \underbrace{\frac{1}{2}\log_2(M)}_{\text{constellation}} + \underbrace{\lfloor \log_2(N_t, N_a) \rfloor}_{\text{spatial}}. \quad (9)$$

In OFDM-based TD-GSM, only the selected N_a LEDs transmit the valid data and the rest of them are unmodulated. As a result, when $N_a < N_t$, OFDM-based TD-GSM suffers from reduced inter-channel-interference (ICI) in comparison to OFDM-based FD-GSM. However, according to (6), if the DC bias we define is relatively small, the output time samples will have a large number of zero samples, which will cause the loss of spatial information. In order to obtain non-zero time domain samples, a secondary bias can be added after clipping so as to guarantee that all the time-domain samples have positive values. Hence, (6) can be modified as

$$s_m = \begin{cases} \epsilon, & x_m < -b \\ x_m + b + \epsilon, & x_m \geq -b \end{cases}, \quad (10)$$

where $\epsilon = \rho b$ is the value of the secondary DC bias with ρ denoting the ratio between the secondary DC bias (i.e., ϵ) and the primary DC bias (i.e., b).

At receiver side, ML detection is performed before OFDM demodulation. The detailed procedures are similar to that of OFDM-based FD-GSM, as given by Algorithm 1, and the main differences are that: (i) the number of elements in $\hat{\mathbf{S}}_T$, $\hat{\mathbf{C}}_T$ and $\hat{\mathbf{x}}_T^{av}$ is increased to N and (ii) we can directly sort the elements of $\hat{\mathbf{s}}_m$ without the need to calculate the moduli.

IV. SIMULATION RESULTS

In this section, we evaluate and compare the performance of OFDM-based FD-GSM and TD-GSM in a typical indoor MIMO-OWC system.

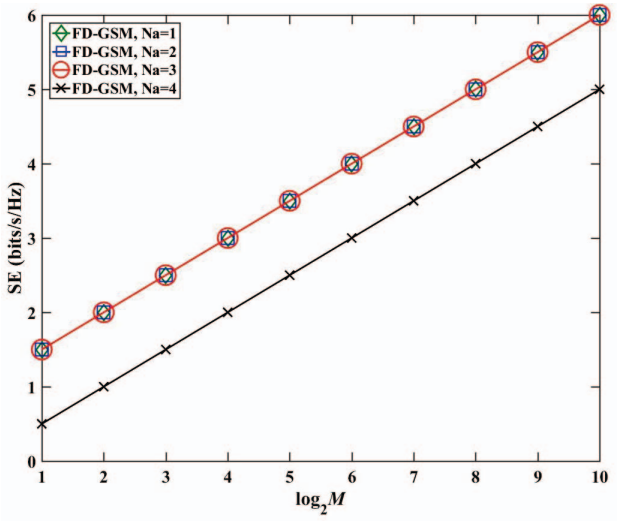

(a) FD-GSM

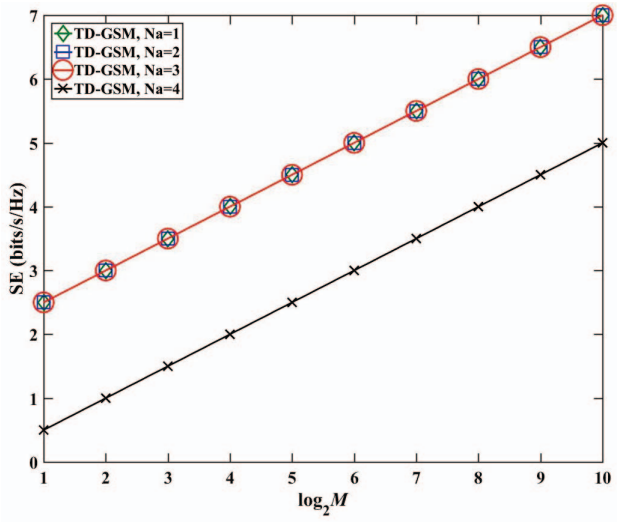

(b) TD-GSM

Fig. 2. Spectral efficiency (bits/s/Hz) vs. $\log_2 M$ for OFDM-based FD-GSM and TD-GSM.

A. Simulation Setup

In our simulations, we consider an indoor 4 × 4 MIMO-OWC system with a dimension of 5 m × 5 m × 3 m, where the LED array is mounted in the ceiling which is 3 m above the floor, and the PD array is located within the receiving plane which is 0.85 m above the floor. The LED array is located at the center of the ceiling and the LED spacing between two adjacent LEDs is 2.5 m while the PD spacing is 10 cm. The position coordinates of the receiver are (2m, 2m, 0.85m). The semi-angle at half power of LED is 60°. The responsivity and active area of PD are 1 A/W and 1 cm^2, respectively. The refractive index and the half-angle FOV of optical lens are 1.5 and 72°, respectively. The signal bandwidth is 20 MHz and

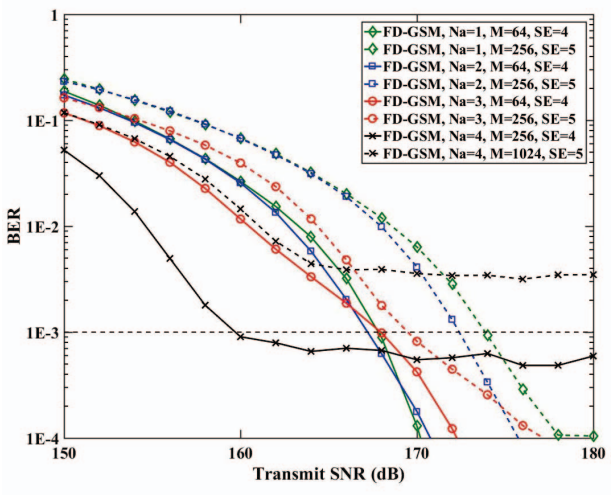

Fig. 3. BER vs. transmit SNR for OFDM-based FD-GSM for different spectral efficiencies (bits/s/Hz).

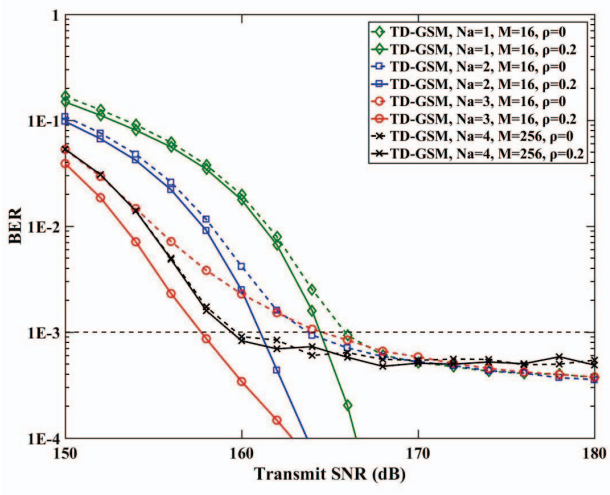

(a) 4 bits/s/Hz

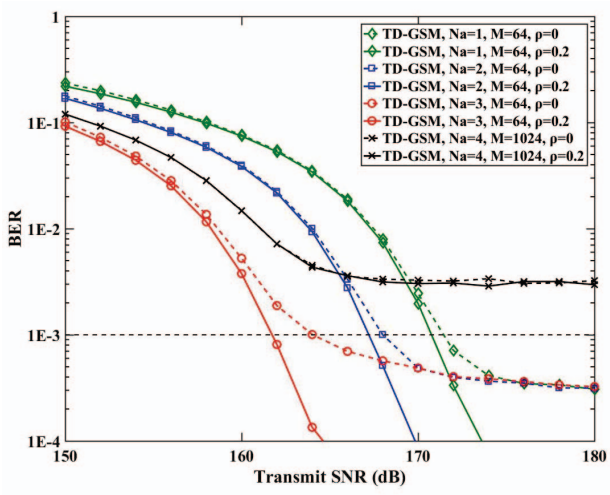

(b) 5 bits/s/Hz

Fig. 4. BER performance vs. transmit SNR for OFDM-based TD-GSM with different spectral efficiency.

the noise PSD is 10^{-22} A^2/Hz. The gain of the optical filter is 0.9. The potential number of activated LEDs is N_a = 1, 2, 3, and 4. The detailed simulation parameters are summarized in Table II.

B. Spectral Efficiency

Figs. 2(a) and (b) show the spectral efficiency versus $\log_2 M$ for OFDM-based FD-GSM and TD-GSM, respectively. In OFDM-based FD-GSM, the achievable spectral efficiencies for N_a = 1 (green line) , 2 (blue line) and 3 (red line) are the same, which are higher than that for N_a = 4. Similarly, OFDM-based TD-GSM with N_a = 1, 2 and 3 achieves the same spectral efficiency and outperforms that for N_a = 4. By comparing Figs. 2(a) and (b), we can see that OFDM-based TD-GSM achieves higher spectral efficiencies than OFDM-based FD-GSM for N_a = 1, 2 and 3, since TD-GSM can get twice as many spatial bits as FD-GSM. When N_a = 4, both FD-GSM and TD-GSM become RC, so they have the same spectral efficiency.

C. BER performance

Fig. 3 shows the BER performance of OFDM-based FD-GSM for different spectral efficiencies, where the DC bias b_{dB} is set to 10 dB. For the spectral efficiency of 4 bits/s/Hz, FD-GSM with N_a = 4 (i.e., RC) has the best BER performance, while FD-GSM with N_a = 1, 2 and 3 achieves comparable BER performance. It can be seen that FD-GSM with N_a = 4 outperforms FD-GSM with N_a = 2 by an SNR gain of 7 dB at BER = 10^{-3}. Moreover, an error floor of about 6.3×10^{-4} occurs for FD-GSM with N_a = 4 when the transmit SNR is relatively large, which is mainly caused by the clipping noise during the OFDM modulation. However, when the spectral efficiency is improved to 5 bits/s/Hz, FD-GSM with N_a = 4 cannot reach the BER of 10^{-3} since its error floor is about 4.4×10^{-3}. In contrast, FD-GSM with N_a = 3 achieves the best BER performance, which outperforms FD-GSM with N_a = 2 by an SNR gain of 2 dB at BER = 10^{-3}.

Fig. 4(a) shows the BER performance of OFDM-based TD-GSM for a spectral efficiency of 4 bits/s/Hz, where the DC bias b_{dB} is 10 dB and two secondary DC bias ratio values ρ = 0 and 0.2 are considered. When ρ = 0, i.e., no secondary DC bias is added, TD-GSM gets the best performance for N_a = 4, while the worst BER performance is obtained by N_a = 1. It can be observed that, for TD-GSM with N_a = 1, 2 and 3, the error floors might occur due to high spatial errors caused by the zero samples in the time domain signals. For TD-GSM with N_a = 4, it also becomes RC and the error floor occurs due to the clipping noise. When ρ = 0.2, the spatial errors can be efficiently reduced and hence the BER performance can be improved. Specifically, TD-GSM with N_a

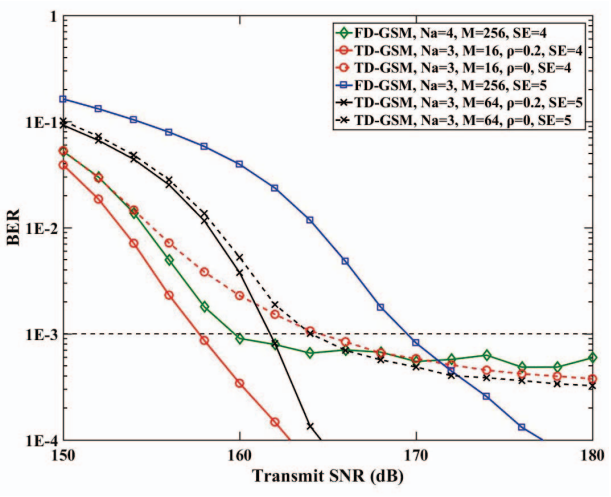

Fig. 5. BER performance comparison between OFDM-based FD-GSM and TD-GSM for different spectral efficiencies (bits/s/Hz).

= 3 achieves the best BER performance, which outperforms N_a = 4 at a BER of 10^{-3} by about 2 dB. It also performs about 3 dB and 6 dB better than N_a = 2 and 1, respectively. Due to the use of a relatively large secondary DC bias, the number of zero samples in the time domain signals is significantly reduced and hence the spatial errors caused by zero samples can be efficiently eliminated. Therefore, the error floors no longer exist for TD-GSM with N_a = 1, 2 and 3. Fig. 4(b) presents the BER performance of OFDM-based TD-GSM for a spectral efficiency of 5 bits/s/Hz, where the DC bias b_{dB} is 10 dB and ρ = 0 and 0.2. As we can observe, TD-GSM with N_a = 4 cannot reach the BER of 10^{-3} with an error floor of about 3.1×10^{-3}, and TD-GSM with N_a = 3 achieves the best BER performance than others for both ρ = 0 and 0.2. When ρ = 0, TD-GSM with N_a = 3 obtains SNR gains of 4 dB and 8 dB at BER = 10^{-3} compared with TD-GSM with N_a = 2 and TD-GSM with N_a = 1, respectively. Moreover, error floors of about 2.9×10^{-4} occur for TD-GSM with N_a = 1, 2 and 3. When ρ = 0.2, TD-GSM with N_a = 3 outperforms TD-GSM N_a = 2 and TD-GSM N_a = 1 by SNR gains of 5 dB and 9 dB at BER = 10^{-3}, respectively. It also can be seen that, for TD-GSM with N_a = 3, an SNR gain of 2 dB is achieved when ρ is increased from 0 to 0.2.

Finally, we compare the BER performance versus transmit SNR between OFDM-based FD-GSM and TD-GSM for different spectral efficiencies, where the optimal value of N_a is selected for each case according to the above results. As we can see, for SE = 4 bits/s/Hz, FD-GSM with N_a = 4 outperforms TD-GSM with N_a = 3 and ρ = 0 by an SNR gain of 5 dB at BER = 10^{-3}. However, TD-GSM with N_a = 3 and ρ = 0.2 performs better than FD-GSM with N_a = 4 with an SNR gain of 2 dB. For the spectral efficiency of 5 bits/s/Hz, whether it has secondary DC bias or not, TD-GSM with N_a = 3 is always superior than FD-GSM with N_a = 3. When ρ = 0, it outperforms FD-GSM with N_a = 3 at a BER of 10^{-3} by an SNR gain of 5 dB, which is increased to 7 dB, when ρ is increased to 0.2.

V. Conclusion

In this paper, we have proposed and evaluated two OFDM-based GSM techniques, including FD-GSM and TD-GSM, for indoor IM/DD MIMO-OWC systems. Compared with conventional SM, multiple LEDs can be selected to transmit the same symbol when applying GSM in the system, which can provide transmit diversity. The obtained simulation results show that, for both OFDM-based FD-GSM and TD-GSM, there exist optimal numbers of the activated OFDM modulators and LED transmitters, respectively. In a typical indoor 4 $\times$ 4 MIMO-OWC system, FD-GSM outperforms TD-GSM without adding a secondary DC bias for a spectral efficiency of 4 bits/s/Hz, while TD-GSM always achieves better BER than FD-GSM when a proper secondary DC bias is applied. In conclusion, OFDM-based FD-GSM might be a promising technique for energy-efficient OWC systems since it does require a secondary DC bias, while OFDM-based TD-GSM has the potential for visible light communication (VLC) systems since a large secondary DC bias is generally required to ensure efficient illumination.

References

[1] T. Cogalan and H. Haas, "Why would 5G need optical wireless communications?" in *Proc. IEEE Ann. Int. Symp. Pers., Indoor Mobile Radio Commun. (PIMRC)*, Oct. 2017, pp. 1–6.

[2] Z. Ghassemlooy, S. Arnon, M. Uysal, Z. Xu, and J. Cheng, "Emerging optical wireless communications-advances and challenges," *IEEE J. Sel. Areas Commun.*, vol. 33, no. 9, pp. 1738–1749, Sep. 2015.

[3] L. Zeng, D. C. O'Brien, H. Le Minh, G. E. Faulkner, K. Lee, D. Jung, Y. Oh, and E. T. Won, "High data rate multiple input multiple output (MIMO) optical wireless communications using white LED lighting," *IEEE J. Sel. Areas Commun.*, vol. 27, no. 9, pp. 1654–1662, Dec. 2009.

[4] T. Fath and H. Haas, "Performance comparison of MIMO techniques for optical wireless communications in indoor environments," *IEEE Trans. Commun.*, vol. 61, no. 2, pp. 733–742, Feb. 2013.

[5] C. Chen, W.-D. Zhong, and D. Wu, "On the coverage of multiple-input multiple-output visible light communications [Invited]," *J. Opt. Commun. Netw.*, vol. 9, no. 9, pp. D31–D41, Sep. 2017.

[6] C. Chen, H. Yang, P. Du, W.-D. Zhong, A. Alphones, Y. Yang, and X. Deng, "User-centric MIMO techniques for indoor visible light communication systems," *IEEE Syst. J.*, vol. 14, no. 3, pp. 3202–3213, Sep. 2020.

[7] R. Mesleh, H. Elgala, and H. Haas, "Optical spatial modulation," *J. Opt. Commun. Netw.*, vol. 3, no. 3, pp. 234–244, Mar. 2011.

[8] X. Zhu, Z. Wang, Q. Wang, and H. Haas, "Virtual spatial modulation for MIMO systems," in *Proc. IEEE Global Commun. Conf. (GLOBECOM)*, Dec. 2016, pp. 1–6.

[9] A. Younis, N. Serafimovski, R. Mesleh, and H. Haas, "Generalised spatial modulation," in *Proc. Signals, Syst. Comput.*, Nov. 2010, pp. 1498–1502.

[10] I. Tavakkolnia, A. Yesilkaya, and H. Haas, "OFDM-Based Spatial Modulation for Optical Wireless Communications," in *Proc. IEEE Globecom Workshops (GC Wkshps)*, Dec. 2018, pp. 1–6.

[11] A. Yesilkaya, R. Bian, I. Tavakkolnia, and H. Haas, "OFDM-based optical spatial modulation," *IEEE J. Sel. Topics Signal Process.*, vol. 13, no. 6, pp. 1433–1444, Jun. 2019.

[12] M. Z. Afgani, H. Haas, H. Elgala, and D. Knipp, "Visible light communication using OFDM," in *Proc. Int. Conf. Testbeds Res. Infrastruct. Develop. Netw. Commun.*, Mar. 2006, pp. 129–134.

[13] S. D. Dissanayake and J. Armstrong, "Comparison of ACO-OFDM, DCO-OFDM and ADO-OFDM in IM/DD Systems," *J. Lightw. Technol.*, vol. 31, no. 7, pp. 1063–1072, Jan. 2013.